Synthesis, characterization and structure determination of two isotypes of a layered aluminophosphate with a new 2D network topology

A. Tuel[a,*], Ch. Lorentz[a], V. Gramlich[b], Ch. Baerlocher[b]

[a]*CNRS, Institut de Recherches sur la Catalyse, 2, avenue A, Einstein, 69626 Villeurbanne Cedex, France*
[b]*Laboratory of Crystallography, ETH Hönggerberg HCI, CH-8093 Zürich, Switzerland*

Abstract

Two isotypes of a new layered aluminophosphate, further denoted MDAP-3 and MDAE-1, have been synthesized under hydrothermal conditions using *N*-methyl-1,3-propanediamine and *N*-methyl-ethylenediamine, respectively. MDAP-3, with the empirical formula $[Al_2(HPO_4)(PO_4)_2](C_4N_2H_{14})(H_2O)$, crystallizes in the orthorhombic space group *Pna*2(1) (No. 33) with $a = 9.602(16)$ Å, $b = 9.26(2)$ Å, $c = 16.03(3)$ Å, $Z = 4$, $R_1 = 0.0498$ and w$R_2 = 0.1217$. The second solid, MDAE-1, with the empirical formula $[Al_2(HPO_4)(PO_4)_2](C_3N_2H_{12})(H_2O)$, crystallizes in the same space group with $a = 9.4250(19)$ Å, $b = 9.3170(19)$ Å, $c = 15.907(3)$ Å, $Z = 4$, $R_1 = 0.0407$ and w$R_2 = 0.0954$. The two compounds possess the same layer topology. Inorganic layers contain $PO_3 = O$, PO_3OH, AlO_4 and AlO_6 polyhedra, linked together to generate a new 4×8 net. MDAP-3 and MDAE-1 represent the first examples of two-dimensional layered aluminophosphates with the $Al_2P_3O_{12}$ stoichiometry, and containing AlO_6 octahedra.
© 2005 Elsevier Inc. All rights reserved.

Keywords: Aluminophosphate; Synthesis; Structure; Template; Diamine

1. Introduction

The discovery of the AlPO$_4$-*n* family in the early 1980s was the starting point of an intense activity in the synthesis of inorganic materials with particular compositions and architectures [1]. Many new crystalline compounds with chains (one-dimensional), layered (two-dimensional) and open framework (three-dimensional) structures have been synthesized and characterized over the last two decades [2]. The family of 2D layered compounds is particularly rich in terms of composition and network topology. Six different stoichiometries have been reported: AlPO$_4$(OH)$^-$ [3–7], AlP$_2$O$_8^{3-}$ [8–10], Al$_2$P$_3$O$_{12}^{3-}$ [11–15], Al$_3$P$_4$O$_{16}^{3-}$ [16–38], Al$_4$P$_5$O$_{20}^{3-}$ [39] and Al$_{13}$P$_{18}$O$_{72}^{15-}$ [40,41]. Except for the Al$_3$P$_4$O$_{16}^{3-}$ stoichiometry, the number of compounds

with other stoichiometries is limited in number. In the case of layered aluminophosphates with P:Al ratio of 3:2, only eight currently known materials have been reported [15]. In this particular family, aluminophosphate sheets are made up of AlO$_4$, AlO$_5$ and PO$_4$ polyhedra, linked together to form six distinct network topologies. All these networks contain 4-membered rings of alternating Al and P polyhedra along with 6-rings and/or 8-rings. These aluminophosphates are obtained in the presence of different types of amines as structure-directing agents. As for other families of 2D-layered aluminophosphates, the role of the amine in the crystallization of a given network topology is not clearly understood. Up to date, aluminophosphates containing sheets with a P:Al ratio of 3:2 have never been obtained in the presence of linear diaminoalkanes.

In the course of our study on the role of diamines in the crystallization of aluminophosphates, we have reported that *N*-methyl-diaminoalkanes could lead to

*Corresponding author. Fax: +33 04 72 44 53 99.

E-mail address: tuel@catalyse.cnrs.fr (A. Tuel).

solids impossible to obtain using the non-substituted corresponding diamines [42]. The present work reports the synthesis and characterization of two new layered aluminophosphates, with a P:Al ratio of 3:2, obtained with *N*-methyl-1,3-propanediamine (further denoted MeDAP) and *N*-methyl-ethylenediamine (further denoted MeDAE). These compounds, which could not be obtained with 1,3-propanediamine and ethylenediamine, respectively, possess the same 2D sheet topology with a new 4×8 net. They represent the first examples of sheets with a P:Al ratio of 3:2 and constructed from PO_4, AlO_4 and AlO_6 polyhedra.

2. Experimental section

2.1. Synthesis

We have previously reported the synthesis of MDAP-1 and MDAP-2, a 2D layered and 3D open-framework aluminophosphates, respectively, using *N*-methyl-1, 3-propanediamine as template [42]. In the present work, MDAP-3 was prepared using the same organic molecule but with a different gel composition. Typically, 5 g of Pseudoboehmite (CATAPAL B, Vista, 74 wt% Al_2O_3) were dispersed in a solution containing 9.8 mL of orthophosphoric acid (H_3PO_4, 85 wt%) and 26 mL of water. The mixture was stirred until homogeneous and

5.3 mL of diamine were added dropwise under vigorous stirring. Stirring was maintained for 2 h and the homogeneous gel, with the composition Al_2O_3–$2P_2O_5$–$1.4MeDAP$–$50H_2O$ was transferred into a 125 mL Teflon-lined stainless-steel autoclave and heated at 180 °C for 24 h under static conditions and autogenous pressure. After crystallization, the solid was recovered by filtration, washed with distilled water and air dried at room temperature. MDAP-3 was obtained pure, in the form of large, doubly terminated, prismatic crystals.

MDAE-1 was prepared following a similar procedure but using 4.45 mL of *N*-methyl-ethylenediamine instead of MeDAP as templating molecule. The solid was also obtained as a pure phase, in the form of large aggregated crystals.

2.2. X-ray data collection and structure determination

For both compounds, a single crystal data set was collected at room temperature with a CAD-4 diffractometer with Mo$K\alpha$ radiation. The structure was solved using SHELX-86 [43] and refined with SHELX-93 [44]. Further details of the data collection and the crystallographic data are given in Table 1. Atomic parameters and selected interatomic distances and bond angles are listed in Tables 2–4. The crystallographic data (excluding structure factors) for these two structures have been

Table 1
Crystal data and structure refinement for MDAP-3 and MDAE-1

Identification code	MDAP-3	MDAE-1
Empirical formula	$[Al_2(HPO_4)(PO_4)_2](C_4N_2H_{14})(H_2O)$	$[Al_2(HPO_4)(PO_4)_2](C_3N_2H_{12})(H_2O)$
Formula weight	448.06	434.04
Temperature (K)	293(2)	293(2)
Wavelength	0.71073 Å	0.71073 Å
Crystal system, space group	Orthorhombic, *Pna*2(1)	Orthorhombic, *Pna*2(1)
Unit cell dimensions	$a = 9.602(16)$ Å	$a = 9.4250(19)$ Å
	$b = 9.26(2)$ Å	$b = 9.3170(19)$ Å
	$c = 16.03(3)$ Å	$c = 15.907(3)$ Å
Volume	1426(5) Å^3	1396.8(5) Å^3
Z	4	4
Calculated density	2.086 Mg/m^3	2.064 Mg/m^3
Absorption coefficient	0.619 mm^{-1}	0.628 mm^{-1}
F (000)	920	888
Crystal size	.09 × .05 × .04 mm	.2 × .1 × .1 mm
Theta range for data collection	2.54–24.97 deg	2.54–24.97 deg
Limiting indices	$0 \leqslant h \leqslant 11$, $0 \leqslant k \leqslant 11$, $-18 \leqslant l \leqslant 0$	$-11 \leqslant h \leqslant 0$, $-11 \leqslant k \leqslant 0$, $-18 \leqslant l \leqslant 0$
Number of reflections ($> 2\sigma(I)$)	750	1070
Reflections collected/unique	1292/1292 [R(int) = 0.0000]	1271/1271 [R(int) = 0.0000]
Completeness to theta = 24.97	99.5%	100.0%
Refinement method	Full-matrix least-squares on F^2	Full-matrix least-squares on F^2
Data/restraints/parameters	1292/5/218	1271/4/218
Goodness-of-fit on F^2	1.121	1.095
Final R indices [$I > 2\sigma(I)$]	$R_1 = 0.0498$, w$R_2 = 0.1217$	$R_1 = 0.0407$, w$R_2 = 0.0954$
R indices (all data)	$R_1 = 0.0525$, w$R_2 = 0.1284$	$R_1 = 0.0583$, w$R_2 = 0.1114$
Absolute structure parameter	0.1(3)	0.2(3)
Largest diff. peak and hole	0.641 and -0.654 e Å^{-3}	0.483 and -0.476 e.Å^{-3}

Table 2
Atomic coordinates ($\times 10^4$) and equivalent isotropic displacement parameters ($\text{Å}^2 \times 10^3$) for MDAP-3 and MDAE-1

	x	y	z	U (eq)
MDAP-3				
P(1)	10029(2)	1114(2)	3430(1)	20(1)
P(2)	8568(2)	5929(2)	2711(1)	22(1)
P(3)	5131(2)	3937(2)	1173(1)	21(1)
Al(1)	10477(2)	8539(2)	2360(1)	22(1)
Al(2)	7709(2)	2712(2)	2296(1)	21(1)
O(1)	11363(4)	1698(5)	3075(3)	29(1)
O(2)	10077(5)	1199(5)	4398(3)	27(2)
O(3)	9878(5)	−520(5)	3233(3)	30(2)
O(4)	8761(5)	1925(5)	3149(3)	30(1)
O(5)	8720(4)	4442(5)	2339(3)	26(1)
O(6)	7268(4)	6700(5)	2380(4)	30(1)
O(7)	8557(5)	5921(5)	3651(3)	30(1)
O(8)	9816(4)	6805(5)	2379(4)	28(1)
O(9)	3956(5)	3040(5)	1495(3)	30(1)
O(10)	6562(5)	3373(5)	1411(3)	31(1)
O(11)	4973(5)	5509(6)	1472(3)	28(2)
O(12)	5052(4)	3944(5)	222(3)	26(2)
O(13W)	6627(5)	857(5)	2232(4)	38(2)
N(1)	7212(6)	−2226(6)	4694(4)	33(2)
C(2)	6866(8)	−901(9)	4231(5)	36(2)
C(4)	5475(8)	481(9)	5348(6)	41(2)
N(5)	4217(6)	992(6)	4881(4)	30(2)
C(6)	2961(8)	1059(9)	5433(5)	44(3)
C(3)	6709(8)	413(8)	4760(6)	38(2)
MDAE-1				
P(1)	9723(2)	1094(2)	3437(1)	11(1)
P(2)	8373(2)	5945(2)	2739(1)	12(1)
P(3)	4927(2)	3942(2)	1155(1)	11(1)
Al(1)	10185(2)	8578(2)	2391(2)	13(1)
Al(2)	7485(2)	2771(2)	2281(2)	11(1)
O(1)	11043(6)	1544(7)	2971(4)	19(1)
O(2)	9930(7)	1220(7)	4399(4)	16(2)
O(3)	9416(7)	−513(6)	3235(4)	20(2)
O(4)	8430(6)	1981(6)	3206(4)	16(1)
O(5)	8543(5)	4451(5)	2345(4)	17(1)
O(6)	6987(6)	6635(6)	2439(5)	29(2)
O(7)	8465(9)	5976(7)	3678(4)	35(2)
O(8)	9564(6)	6835(5)	2323(5)	21(1)
O(9)	3825(7)	2948(6)	1517(4)	17(2)
O(10)	6417(6)	3415(7)	1325(4)	16(1)
O(11)	4737(7)	5493(7)	1477(4)	21(2)
O(12)	4730(7)	3993(7)	192(4)	20(2)
O(13W)	6421(7)	946(7)	2182(5)	24(2)
N(1)	7223(9)	−1898(9)	4733(5)	29(2)
C(2)	6540(12)	−546(12)	4519(7)	38(3)
C(3)	5461(11)	−88(12)	5175(7)	34(3)
N(4)	4397(8)	898(8)	4813(5)	21(2)
C(5)	3219(11)	1241(12)	5388(8)	42(3)

U (eq) is defined as one third of the trace of the orthogonalized U_{ij} tensor.

deposited with the Cambridge Crystallographic Data Centre as supplementary publication nos. CCDC 265038 and 265039 for MDAE-1 and MDAP-3, respectively. Copies of the data can be obtained, free of charge, on application to CCDC, 12 Union Road, Cambridge CB2 1EZ, UK, (fax: +44 1223 336033 or e-mail: deposit@ccdc.cam.ac.uk).

Table 3
Bond lengths (Å) and angles (deg) for MDAP-3

P(1)–O(4)	1.500(5)
P(1–O(1)	1.503(5)
P(1)–O(3)	1.553(6)
P(1)–O(2)	1.554(7)
P(2)–O(7)	1.508(6)
P(2)–O(5)	1.508(6)
P(2)–O(6)	1.533(5)
P(2)–O(8)	1.542(5)
P(3)–O(9)	1.494(5)
P(3)–O(10)	1.518(5)
P(3)–O(12)	1.527(7)
P(3)–O(11)	1.541(7)
Al(1)–O(8)	1.727(6)
Al(1)–O(6)#1	1.734(5)
Al(1)–O(11)#1	1.742(6)
Al(1)–O(3)#2	1.748(6)
Al(2)–O(4)	1.850(6)
Al(2)–O(5)	1.874(6)
Al(2)–O(1)#3	1.879(6)
Al(2)–O(9)#4	1.889(5)
Al(2)–O(10)	1.898(6)
Al(2)–O(13W)	2.011(6)
O(1)–Al(2)#4	1.879(6)
O(3)–Al(1)#5	1.747(6)
O(6)–Al(1)#6	1.734(5)
O(9)–Al(2)#3	1.889(5)
O(11)–Al(1)#6	1.743(6)
N(1)–C(2)	1.472(10)
C(2)–C(3)	1.492(12)
C(4)–N(5)	1.498(10)
C(4)–C(3)	1.515(12)
N(5)–C(6)	1.498(10)
O(4)–P(1)–O(1)	113.4(3)
O(4)–P(1)–O(3)	110.6(3)
O(1)–P(1)–O(3)	110.7(3)
O(4)–P(1)–O(2)	107.4(3)
O(1)–P(1)–O(2)	109.6(3)
O(3)–P(1)–O(2)	104.8(3)
O(7)–P(2)–O(5)	113.0(3)
O(7)–P(2)–O(6)	110.1(3)
O(5)–P(2)–O(6)	111.6(3)
O(7)–P(2)–O(8)	110.6(3)
O(5)–P(2)–O(8)	105.6(3)
O(6)–P(2)–O(8)	105.6(3)
O(9)–P(3)–O(10)	113.9(3)
O(9)–P(3)–O(12)	108.0(3)
O(10)–P(3)–O(12)	107.3(3)
O(9)–P(3)–O(11)	110.1(3)
O(10)–P(3)–O(11)	109.7(3)
O(12)–P(3)–O(11)	107.6(3)
O(8)–Al(1)–O(6)#1	104.2(2)
O(8)–Al(1)–O(11)#1	112.6(3)
O(6)#1–Al(1)–O(11)#1	110.8(3)
O(8)–Al(1)–O(3)#2	109.2(3)
O(6)#1–Al(1)–O(3)#2	112.0(3)
O(11)#1–Al(1)–O(3)#2	108.1(3)
O(4)–Al(2)–O(5)	91.6(2)
O(4)–Al(2)–O(1)#3	89.9(3)
O(5)–Al(2)–O(1)#3	94.8(2)
O(4)–Al(2)–O(9)#4	90.7(3)
O(5)–Al(2)–O(9)#4	90.7(2)
O(1)#3–Al(2)–O(9)#4	174.5(2)
O(4)–Al(2)–O(10)	175.4(2)
O(5)–Al(2)–O(10)	93.0(3)

Table 3 (*continued*)

O(1)#3–Al(2)–O(10)	90.2(3)
O(9)#4–Al(2)–O(10)	88.7(3)
O(4)–Al(2)–O(13W)	89.0(3)
O(5)–Al(2)–O(13W)	179.2(3)
O(1)#3–Al(2)–O(13W)	85.8(2)
O(9)#4–Al(2)–O(13W)	88.7(3)
O(10)–Al(2)–O(13W)	86.4(2)
P(1)–O(1)–Al(2)#4	160.6(4)
P(1)–O(3)–Al(1)#5	128.2(3)
P(1)–O(4)–Al(2)	149.6(4)
P(2)–O(5)–Al(2)	138.2(3)
P(2)–O(6)–Al(1)#6	139.0(3)
P(2)–O(8)–Al(1)	141.4(3)
P(3)–O(9)–Al(2)#3	156.8(3)
P(3)–O(10)–Al(2)	145.5(3)
P(3)–O(11)–Al(1)#6	134.8(3)
N(1)–C(2)–C(3)	114.6(7)
N(5)–C(4)–C(3)	109.5(7)
C(6)–N(5)–C(4)	111.5(6)
C(2)–C(3)–C(4)	117.8(7)

Symmetry transformations used to generate equivalent atoms: #1 $x+1/2,-y+3/2,z$ #2 $x,y+1,z$ #3 $x-1/2,-y+1/2,z$; #4 $x+1/2,-y+1/2,z$ #5 $x,y-1,z$ #6 $x-1/2,-y+3/2,z$.

Table 4
Bond lengths (Å) and angles (deg) for MDAE-1

P(1)–O(1)	1.507(6)
P(1)–O(4)	1.518(6)
P(1)–O(2)	1.547(7)
P(1)–O(3)	1.559(6)
P(2)–O(7)	1.497(7)
P(2)–O(6)	1.532(6)
P(2)–O(5)	1.535(5)
P(2)–O(8)	1.545(6)
P(3)–O(9)	1.506(6)
P(3)–O(10)	1.512(6)
P(3)–O(11)	1.543(7)
P(3)–O(12)	1.544(7)
Al(1)–O(6)#1	1.712(6)
Al(1)–O(8)	1.729(5)
Al(1)–O(11)#1	1.744(7)
Al(1)–O(3)#2	1.745(6)
Al(2)–O(5)	1.859(5)
Al(2)–O(1)#3	1.860(6)
Al(2)–O(4)	1.870(6)
Al(2)–O(9)#4	1.877(6)
Al(2)–O(10)	1.921(6)
Al(2)–O(13W)	1.980(7)
O(1)–Al(2)#4	1.860(6)
O(3)–Al(1)#5	1.745(6)
O(6)–Al(1)#6	1.712(6)
O(9)–Al(2)#3	1.877(6)
O(11)–Al(1)#6	1.744(7)
N(1)–C(2)	1.455(13)
C(2)–C(3)	1.518(14)
C(3)–N(4)	1.476(12)
N(4)–C(5)	1.473(13)
O(1)–P(1)–O(4)	113.1(4)
O(1)–P(1)–O(2)	111.2(4)
O(4)–P(1)–O(2)	107.5(4)
O(1)–P(1)–O(3)	108.6(4)
O(4)–P(1)–O(3)	108.9(4)

Table 4 (*continued*)

O(2)–P(1)–O(3)	107.4(3)
O(7)–P(2)–O(6)	110.6(4)
O(7)–P(2)–O(5)	114.8(4)
O(6)–P(2)–O(5)	110.0(3)
O(7)–P(2)–O(8)	112.0(4)
O(6)–P(2)–O(8)	105.1(4)
O(5)–P(2)–O(8)	103.7(3)
O(9)–P(3)–O(10)	111.9(4)
O(9)–P(3)–O(11)	111.7(4)
O(10)–P(3)–O(11)	110.6(4)
O(9)–P(3)–O(12)	108.3(4)
O(10)–P(3)–O(12)	107.4(4)
O(11)–P(3)–O(12)	106.7(4)
O(6)#1–Al(1)–O(8)	103.3(3)
O(6)#1–Al(1)–O(11)#1	109.6(4)
O(8)–Al(1)–O(11)#1	109.4(4)
O(6)#1–Al(1)–O(3)#2	115.7(4)
O(8)–Al(1)–O(3)#2	111.3(3)
O(11)#1–Al(1)–O(3)#2	107.4(3)
O(5)–Al(2)–O(1)#3	94.0(3)
O(5)–Al(2)–O(4)	91.9(3)
O(1)#3–Al(2)–O(4)	91.1(3)
O(5)–Al(2)–O(9)#4	88.6(3)
O(1)#3–Al(2)–O(9)#4	175.2(3)
O(4)–Al(2)–O(9)#4	92.8(3)
O(5)–Al(2)–O(10)	93.5(3)
O(1)#3–Al(2)–O(10)	88.7(3)
O(4)–Al(2)–O(10)	174.6(3)
O(9)#4–Al(2)–O(10)	87.2(3)
O(5)–Al(2)–O(13W)	177.6(3)
O(1)#3–Al(2)–O(13W)	88.4(3)
O(4)–Al(2)–O(13W)	88.0(3)
O(9)#4–Al(2)–O(13W)	89.0(3)
O(10)–Al(2)–O(13W)	86.6(3)
P(1)–O(1)–Al(2)#4	171.3(4)
P(1)–O(3)–Al(1)#5	123.2(4)
P(1)–O(4)–Al(2)	141.9(4)
P(2)–O(5)–Al(2)	136.9(4)
P(2)–O(6)–Al(1)#6	144.2(4)
P(2)–O(8)–Al(1)	136.3(4)
P(3)–O(9)–Al(2)#3	158.6(4)
P(3)–O(10)–Al(2)	136.8(4)
P(3)–O(11)–Al(1)#6	135.5(4)
N(1)–C(2)–C(3)	112.3(8)
N(4)–C(3)–C(2)	111.2(8)
C(5)–N(4)–C(3)	113.9(8)

Symmetry transformations used to generate equivalent atoms: #1 $x+1/2,-y+3/2,z$ #2 $x,y+1,z$ #3 $x-1/2,-y+1/2,z$; #4 $x+1/2,-y+1/2,z$ #5 $x,y-1,z$ #6 $x-1/2,-y+3/2,z$.

2.3. Characterization

Thermal analysis data were recorded on a Setaram TGDT A92 apparatus. Samples were heated in air from 25 to 750 °C at a heating rate of 5 °C/min.

Solid-state magic angle spinning (MAS) NMR spectra were acquired on a Bruker DSX 400 spectrometer operating at 104.2 and 161.2 MHz for [27]Al and ^{31}P nuclei, respectively. Samples were spun at 11 kHz at the magic angle in a double-bearing 4 mm probe head. The pulse lengths were 2 μs ($\pi/4$) and 0.7 μs ($\pi/6$), and

the recycle delays were 30 and 1s for ^{31}P and ^{27}Al nuclei, respectively. ^{31}P and ^{27}Al chemical shifts were referenced to H_3PO_4 (85 wt%) and $Al(H_2O)_6^{3+}$, respectively.

Two dimensional-five quanta (2D-5Q) ^{27}Al MAS NMR spectra were collected at 14 kHz using the two-pulse sequence originally reported by Medek et al. [45] and further modified by Fernandez and Amoureux [46] for the study of $S = 5/2$ nuclei. In total, 320 scans were accumulated for each free induction decay with a recycle delay of 500 ms. A total of 128 time-domain real data points were acquired in the indirect dimension, and pure phase spectra were obtained using the TPPI scheme [47,48]. A shearing transformation was applied to the spectra in order to obtain isotropic projections parallel to the f_1 direction.

^{27}Al-^{31}P CP/MAS experiments were carried out using a three-channel ^{1}H-X-Y probe head and a conventional spin lock sequence. 2D ^{27}Al-^{31}P CP/MAS NMR spectra were obtained by encoding the aluminum evolution frequencies in an initial time period after the 90° pulse. Pure absorption phase NMR line shapes in both dimensions were obtained by cycling the phase of the 90° pulse using the TPPI scheme [47,48]. A more homogeneous polarization transfer was achieved by linear amplitude modulation of the spin-lock field on aluminum. The contact time was 1.5 ms and the recycle delay was 300 ms. In a typical experiment, 2048 scans were accumulated for each of the 64 time-domain data points acquired in the aluminum dimension.

3. Results and discussion

3.1. Structure and characterization of MDAP-3

The structure of the two compounds consists of aluminophosphate layers separated by and connected to doubly protonated diamine molecules. The unit cell contains three crystallographically non-equivalent P sites and two non-equivalent Al sites (Fig. 1). The 3 crystallographically distinct P atoms share three oxygens with adjacent Al atoms in the layer. Two of them, based on P(2) and P(3), possess a terminal P=O double bond whilst the third, based on P(1), has a terminal P-OH group. One of the two crystallographically distinct Al atoms Al(1) is tetrahedrally coordinated and bonded to one P(1), one P(3) and two P(2) atoms. Al–O bond lengths and O–Al–O bond angle values are in the range of 1.727(6)–1.748(6) Å and 104.2(2)–112.6(3)°, respectively, which are typical of four-coordinate Al atoms in crystalline aluminophosphates (Table 3). Very similar values are found in MDAE-1 obtained using *N*-methylethylenediamine as structure-directing molecule (Table 4). The other aluminum atom Al(2) is 6-coordinate and connects one P(2), two P(1) and two P(3) atoms. The
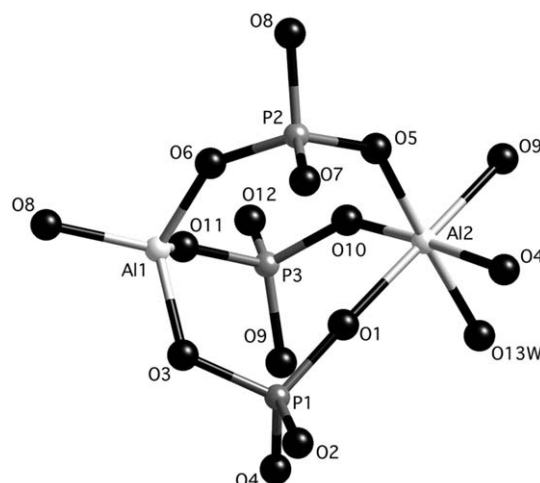

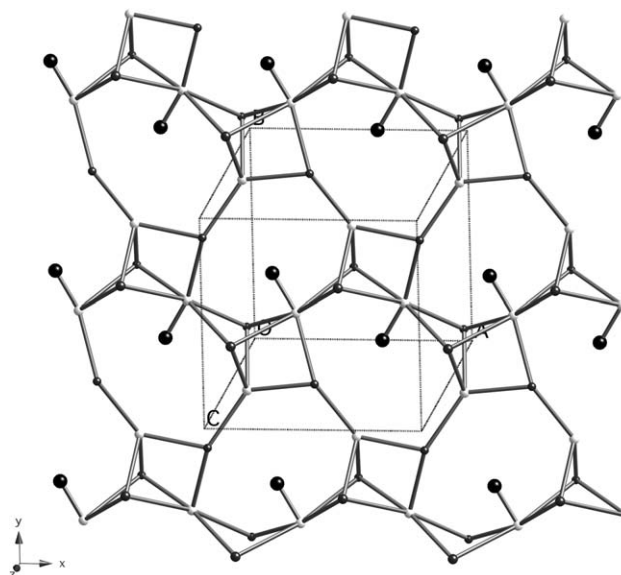Fig. 1. Local coordination of the framework atoms in the two compounds.

Fig. 2. View along the *c*-axis of the inorganic layers in MDAP-3. All oxygen atoms have been omitted, except the oxygen O13W of the water molecule (large black spheres).

sixth ligand is a water molecule located in an 8-ring unit of the layer. P tetrahedra and Al polyhedra alternate to form a (4 × 8) net parallel to the ab plane (Figs. 2 and 3). This net has never been previously reported for layered aluminophosphates with $Al_2P_3O_{12}^{3-}$ stoichiometry. The sheet structure is constructed from the primary building unit shown in Fig. 1. All already known amine-templated aluminophosphates with $Al_2P_3O_{12}^{3-}$ stoichiometry contain different primary building units. Indeed, in all other compounds, the two crystallographically non-equivalent Al atoms form 4-MR units with two P atoms, the units being connected to one another by the third phosphorus atom [13]. In MDAP-3, Al1 and Al2
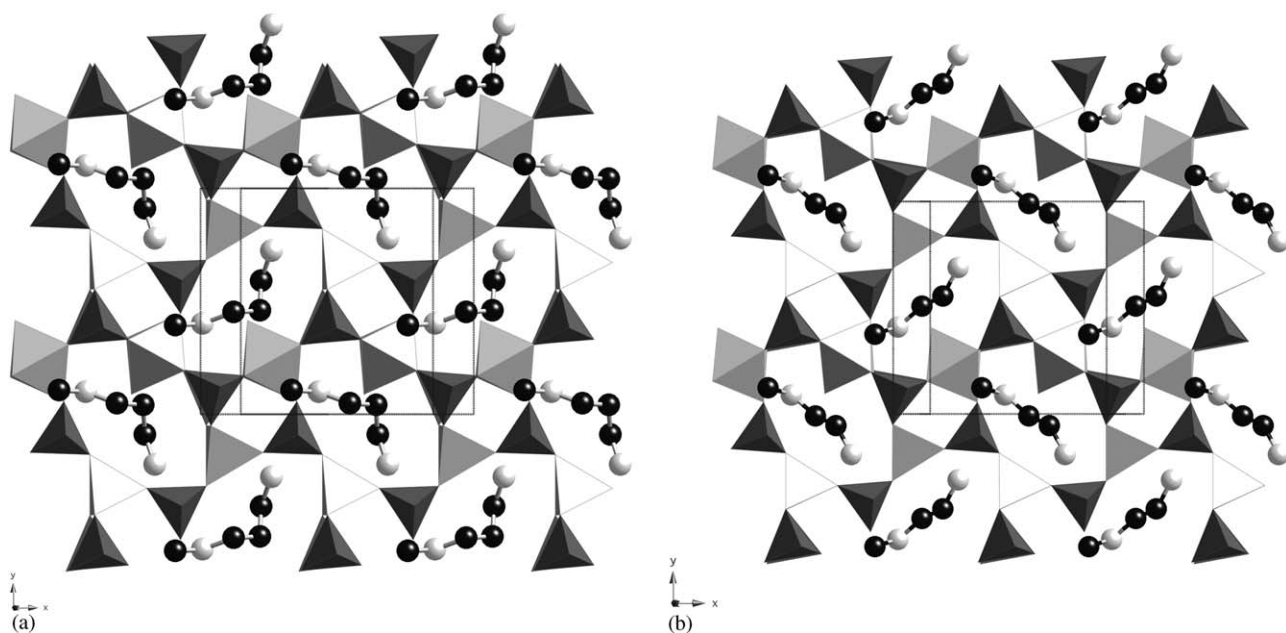
Fig. 3. View along the *c*-axis of the structure of MDAP-3 (a) and MDAE-1 (b). Key: dark gray tetrahedra = P; light gray polyhedra: Al; black spheres : C; white spheres : N.

are bridged by the 3 crystallographically non-equivalent P atoms, leading to a primary unit made of three different 4-MRs. The diversity of 2D networks with $Al_2P_3O_{12}^{3-}$ stoichiometry depends not only on the arrangement of the building units, but also on the coordination of Al atoms in the latter. Up to date, structures containing units with 2 AlO_4, one AlO_4 and one AlO_5 or two AlO_5 polyhedra have been reported [15]. The two compounds described in the present work constitute the first example of structures built-up from primary units containing AlO_6 octahedra. The sheet structure can also be viewed as an alternation of two types of chains running along the *a*-axis (Fig. 2). The first type with $AlP_2O_8(H_2O)$ stoichiometry contains only 6-coordinate Al species. These chains are cross-linked by $AlPO_4$ chains, also running along the *a*-axis, and containing exclusively AlO_4 and $PO_3(=O)$ tetrahedra.

The negative charge on aluminophosphate layers is balanced by doubly protonated *N*-methyl-1,3-propane-diamine molecules. These molecules not only act as space-fillers or charge balancers but they also serve as hydrogen-bonding donors to nearest framework oxygens. A network of H-bonding, between oxygen atoms protruding into the interlayer region and nitrogen atoms of the template, hold the inorganic sheets together. The N(1) atom of MeDAP molecules forms two bonds to oxygen atoms in the upper layer and one bond to the oxygen atom of a P(2)=O(7) group in the lower layer (Fig. 4a). In the upper layer, the two O atoms belong to P(3)=O(12) groups with a N(1)…O(12) distance of

2.966 and 2.825 Å. There are two additional contacts in the upper layer with the slightly more distant bridging oxygens O(9) and O(10), with N(1)…O(9) and N(1)…O(10) distances of 3.19(3) and 3.04(3) Å, respectively. The N(5) atom is involved in two H-bond interactions with one P(1)–O(2)H(2) and one P(2)=O(7) groups, both located in the lower layer. Layers are also held together by a hydrogen bond between oxygen atoms of P(1)–O(2)H(2) and P(3)=O(12) groups in adjacent sheets with a O(2)…O(12) distance of 2.47(2) Å and a O(2)–H(2)–O(12) angle of 164.5°. There is also one intra-sheet hydrogen bond of 2.81(2) Å between the oxygen atom of the water molecule O(13W) and a framework oxygen O(5) (Fig. 4a).

The P:Al ratio of the bulk sample, determined by chemical analysis, was 1.48 for MDAP-3 (1.51 for MDAE-1), in excellent agreement with that expected on the basis of the crystal structure (P/Al = 1.5). Moreover, heating the solid in air up to 750 °C gave a weight loss of ca. 19.1 wt%, very close to the organic content of the crystals (19.3 wt%). The ^{27}Al MAS NMR spectrum of MDAP-3 is composed of two asymmetric signals at 40 and −30 ppm with a relative intensity of 1:1 (Fig. 5). They can be assigned to the tetrahedral Al(2) and octahedral Al(1) species, respectively. A 2D-5Q MAS spectrum showed that both lines correspond to a unique Al site, in agreement with the 2 crystallographically distinct sites in the structure. The ^{31}P MAS NMR spectrum shows three peaks at −16, −18 and −21 ppm, which correspond to the three crystallographically non-equivalent P sites of the structure. By contrast to ^{27}Al
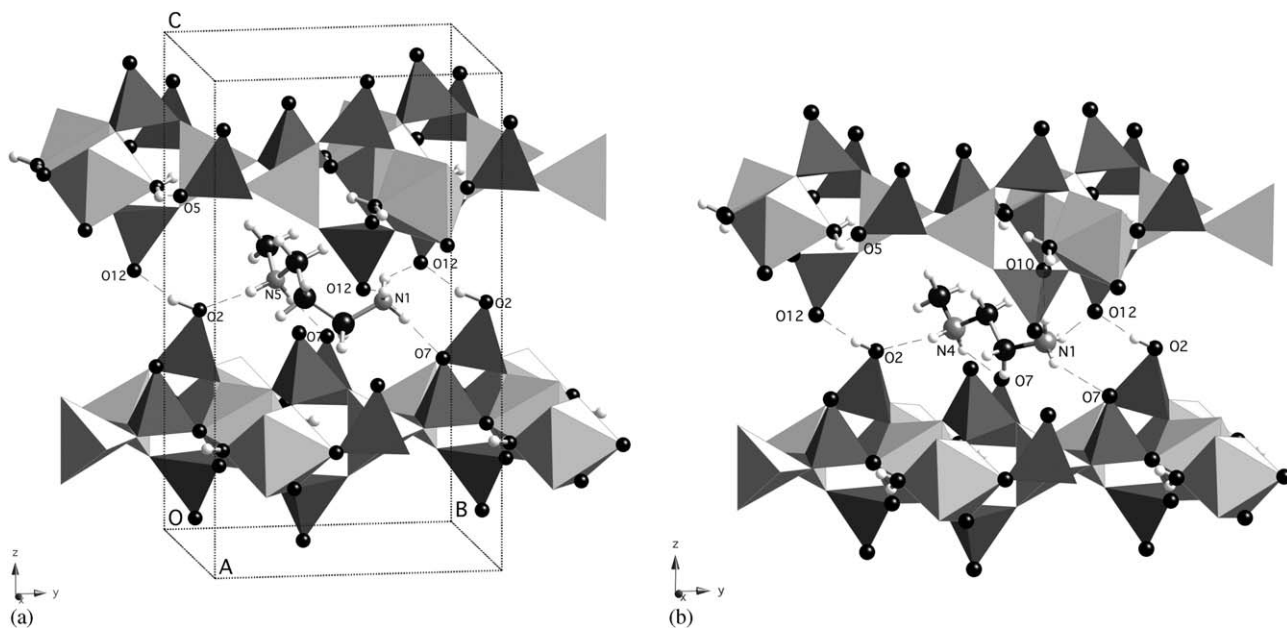
Fig. 4. Hydrogen bond interactions between organic molecules and inorganic layers in MDAP-3 (a) and MDAE-1 (b). Intra and interlayer H-bonds are represented as dashed lines.
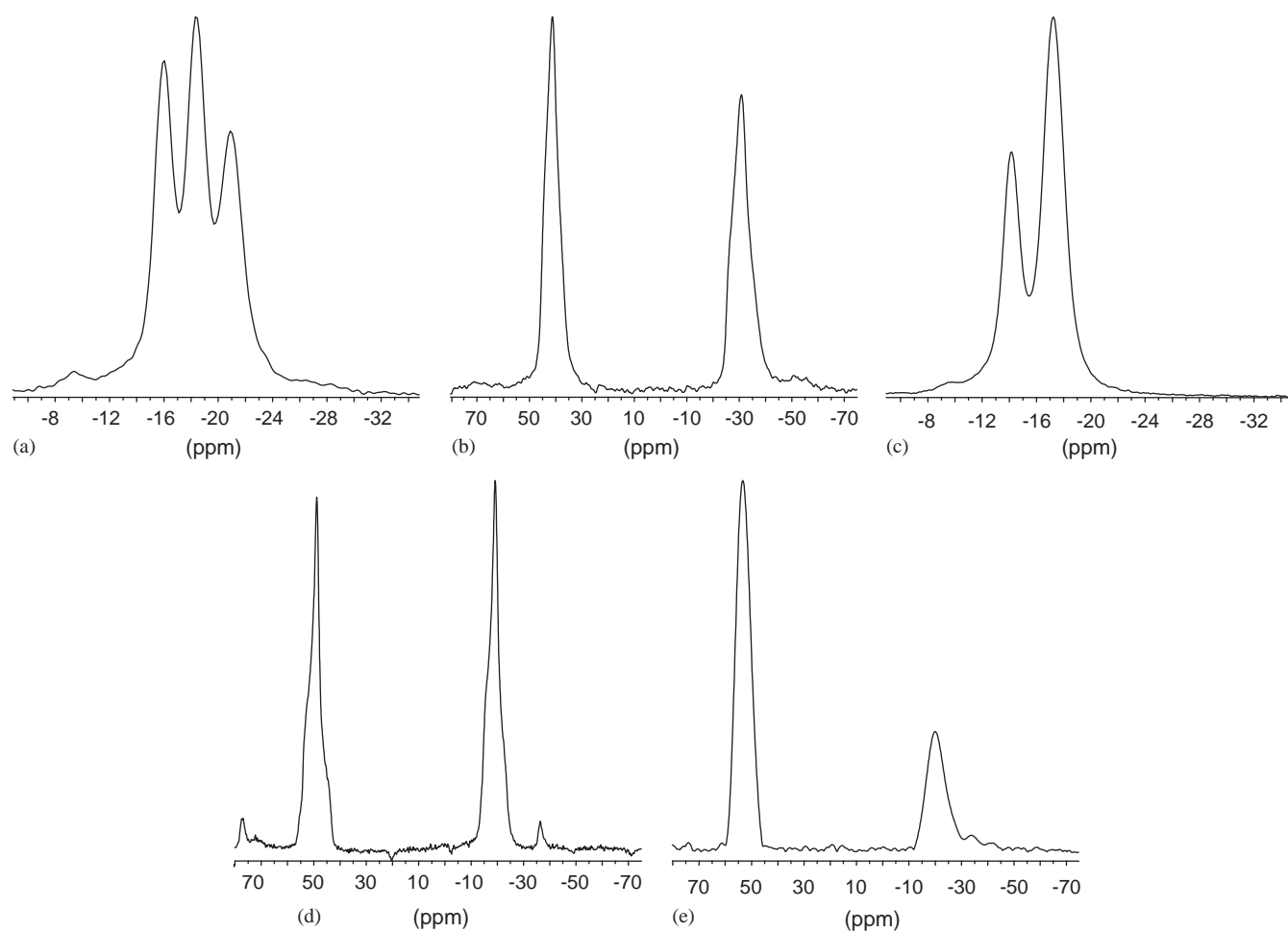

Fig. 5. ^{31}P and ^{27}Al MAS NMR spectra of MDAP-3 (a, b) and MDAE-1 (c, d). Spectrum (e) is the projection in the isotropic dimension of the ^{27}Al 2D-5Q MAS spectrum of MDAE-1.

signals, the assignment of ^{31}P lines is not straightforward because all P atoms are 4-coordinate and the chemical shift variation is quite small. Many semi quantitative correlations between a geometrical parameter around a P atom and the corresponding chemical shift have been used to assign ^{31}P NMR signals in aluminophosphates. For example, Müller et al. proposed that the ^{31}P chemical shift in 3-dimensional AlPO$_4$ compounds is proportional to the mean P–O–Al bond angle value in the structure [49]. In MDAP-3, the mean $\langle$P–O–Al$\rangle$ bond angle values are 145.5, 139.2 and 143.6° for P(1), P(2) and P(3), respectively (Table 3). We have already reported that such a relationship is also valid for PO$_3$(=O) tetrahedra in layered compounds [34]. Thus, NMR signals at −16, −18 and −21 ppm can be reasonably assigned to P(2), P(3) and P(1), respectively. Two-dimensional ^{27}Al-^{31}P CP/MAS NMR supports this assignment. The ^{27}Al-^{31}P NMR correlation spectrum (Fig. 6) gives direct indication about chemical bonding in the structure. In AlPO sheets, P(1) and P(3) are both bonded to one tetrahedral Al(1) and two octahedral Al(2), whilst P(2) is connected to two Al(1) and one Al(2). Thus, all three phosphorus atoms are connected to the two types of Al atoms, making the assignment difficult. However, ^{31}P signals can be partly assigned by looking at the corresponding traces in the f$_1$ dimension. Traces corresponding to ^{31}P NMR signals at −18 and −21 ppm are very similar and show an intense signal at 50 ppm along with a weaker line around −25 ppm. These ^{31}P NMR signals correspond to P(1) and P(3), for which structure connectivities are identical. By contrast, the relative intensities of ^{27}Al signals at 50 and −25 ppm in the trace at −16 ppm are different. Although NMR signals obtained using a cross-polariza-

tion technique are not directly proportional to the number of resonating nuclei, the difference with traces at −18 and −21 ppm is significant enough to be sure that the structural environment of the corresponding P atom is different. In particular, the relatively small intensity of the signal at −25 ppm in the f$_1$ dimension indicates that P is bonded to only one octahedral Al(2) and can be unambiguously assigned to P(2). Moreover, the trace at 50 ppm corresponding to tetrahedral aluminum shows 3 peaks at −16, −18 and −21 ppm, confirming that Al(1) is bonded to the three crystallographically distinct P atoms in the structure. Comparing the intensities of these three lines with those of the ^{31}P MAS spectrum (Fig. 5) clearly shows that the polarization transfer is more efficient for the phosphorus species resonating at −16 ppm. Once more, this suggests that this species is bonded to two Al(1) whilst the others are bonded to one Al(1).

3.2. Structure and characterization of MDAE-1

The nature of the organic amine has minor influence on the structure of the solid. As an example, the unit cell parameters of MDAE-1 are very similar to those of MDAP-3 (Table 1). The main difference concerns the location of organic molecules between the layers and their interaction with framework oxygen. From Fig. 3b, one can see that N-methyl-ethylenediamine molecules arrange so that N atoms occupy approximately the same position as in MDAP-3. However, the orientation of the molecule is slightly different, which affects the H-bond scheme between the terminal N atom and inorganic layers. For the internal nitrogen atom N(4) the hydrogen bond scheme is the same as that of N(5) in
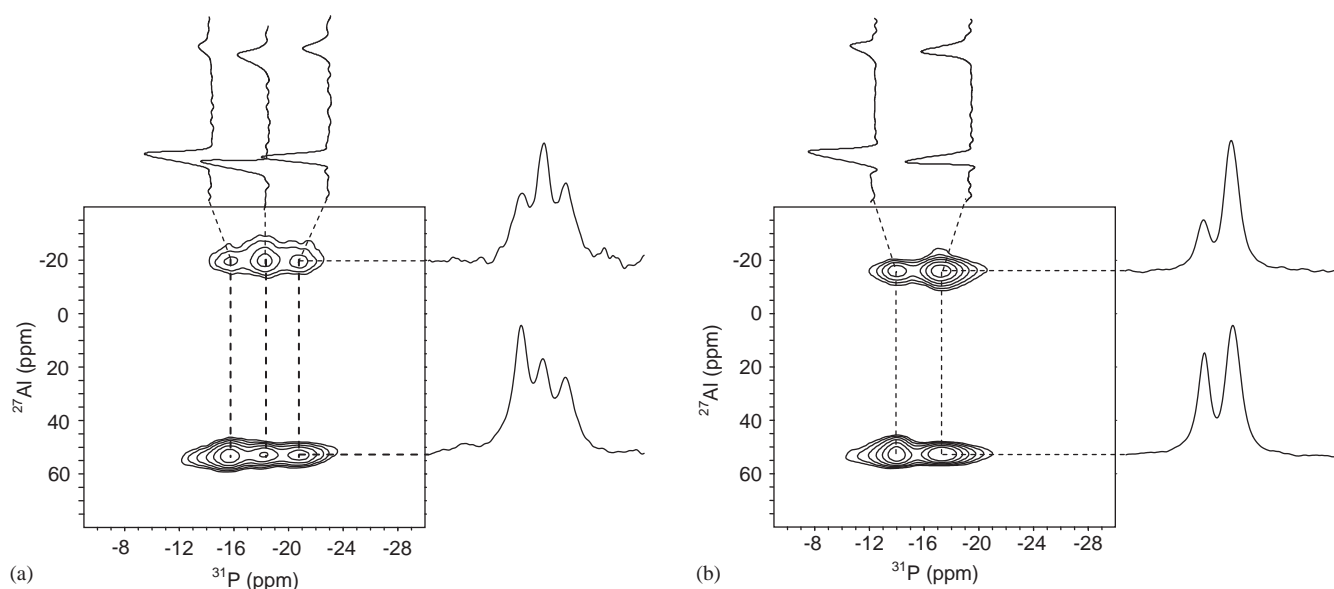

Fig. 6. ^{27}Al-^{31}P CP/MAS correlation spectra of MDAP-3 (a) and MDAE-1 (b).

MeDAP (Fig. 4b). The terminal N(1) atom has three contacts with two O atoms in the upper layer (O(10) and O(12)) and one in the lower layer (O(7)). By contrast to MDAP-3, there is only one additional H-bond with a more distant oxygen in the upper layer, with a N(1)…O(12) distance of 3.08(3) Å.

The ^{27}Al MAS NMR spectrum of MDAE-1 is composed of two signals at 50 and -25 ppm. As for MDAP-3, they are assigned to the two crystallographically distinct Al sites in the structure (Fig. 5). By contrast, the ^{31}P NMR spectrum shows only two lines at ca. -14 and -18 ppm, with a relative intensity of 1:2. A partial assignment can be obtained from ^{27}Al-^{31}P CP/MAS NMR data (Fig. 6). The ^{27}Al trace corresponding to the P atom at -14 ppm is composed of an intense peak at 50 ppm along with a smaller resonance at -15 ppm. The other P atoms also show two ^{27}Al correlation peaks at 50 and -15 ppm in the indirect dimension, but the peak at -15 ppm is approximately 3 times more intense than that corresponding to the phosphorus resonating at -14 ppm. Thus, the ^{31}P NMR signal at -14 ppm corresponds to the phosphorus atom of the structure bonded to only one octahedral aluminum, i.e., P2. As a consequence, the line at -18 ppm has to be assigned to P1 and P3. Again, this assignment was supported by the values of the mean $\langle$P–O–Al$\rangle$ bond angle. The value corresponding to the phosphorus atom P2 (139.1°) is significantly lower than those corresponding to P1 and P3 (144.1° and 143.5°, respectively). The difference in bond angle between P1 and P3, which is only 0.6° (it was 1.9° for MDAP-3), could explain why the two NMR signals are superimposed in the spectrum of MDAE-1.

References

[1] S.T. Wilson, B.M. Lok, C.A. Messina, T.R. Cannan, E.M. Flanigen, J. Am. Chem. Soc. 104 (1982) 1146.

[2] J. Yu, R. Xu, Acc. Chem. Res. 36 (2003) 481.

[3] S. Cheng, J.N. Tzeng, B.Y. Hsu, Chem. Mater. 9 (1997) 1788.

[4] K.O. Kongshaug, H. Fjellvag, K.P. Lillerud, Microporous Mesoporous Mater. 32 (1999) 17.

[5] K.O. Kongshaug, H. Fjellvag, K.P. Lillerud, J. Mater. Chem. 9 (1999) 1591.

[6] H. Yuan, J. Chen, Z. Shi, W. Chen, Y. Wang, P. Zhang, J. Yu, R. Xu, J. Chem. Soc. Dalton Trans. (2000) 1981.

[7] K. Maeda, A. Tuel, C.J. Baerlocher, J. Chem. Soc. Dalton Trans. (2000) 2457.

[8] K.R. Morgan, G.J. Gainsford, N.B. Milestone, Chem. Commun. (1997) 61.

[9] J. Yu, I.D. Williams, J. Solid State Chem. 136 (1998) 141.

[10] M.A. Leech, A.R. Cowley, K. Prout, A.M. Chippindale, Chem. Mater. 10 (1998) 451.

[11] A.M. Chippindale, A.V. Powell, L.M. Bull, R.H. Jones, A.K. Cheetham, J.M. Thomas, R. Xu, J. Solid State Chem. 96 (1992) 199.

[12] S. Oliver, A. Kuperman, A. Lough, G.A. Ozin, Chem. Commun. (1996) 1761.

[13] J. Yu, K. Sugiyama, K. Hiraga, N. Togashi, O. Terasaki, Y. Tanaka, S. Nakata, S. Qiu, R. Xu, Chem. Mater. 10 (1998) 3636.

[14] P. Lightfoot, Z.A.D. Lethbridge, R.E. Morris, D.S. Wragg, P.A. Wright, A. Kvick, G.B.M. Vaughan, J. Solid State Chem. 143 (1999) 74.

[15] A.M. Chippindale, R.I. Walton, J. Solid State Chem. 145 (1999) 731.

[16] R.H. Jones, J.M. Thomas, R. Xu, Q. Huo, A.K. Cheetham, A.V.J. Powell, J. Chem. Soc. Chem. Commun. (1991) 1266.

[17] A.M. Chippindale, A.V. Powell, L.M. Bull, R.H. Jones, A.K. Cheetham, J.M. Thomas, R. Xu, J. Solid State Chem. 96 (1992) 199.

[18] J.M. Thomas, R.H. Jones, R. Xu, J. Chen, A.M. Chippindale, S. Natarajan, A.K. Cheetham, J. Chem. Soc. Chem. Commun. (1992) 929.

[19] R.H. Jones, A.M. Chippindale, S. Natarajan, J.M. Thomas, J. Chem. Soc. Chem. Commun. (1994) 565.

[20] K.R. Morgan, G. Gainsford, N.J. Millestone, J. Chem. Soc. Chem. Commun. (1995) 425.

[21] P.A. Barrett, R.H. Jones, J. Chem. Soc. Chem. Commun. (1995) 1979.

[22] D.A. Bruce, A.P. Wilkinson, M.G. White, J.A. Bertrand, J. Chem. Soc. Chem. Commun. (1995) 2059.

[23] I.D. Williams, Q. Gao, J. Chen, L. Ngai, Z. Lin, R. Xu, Chem. Commun. (1996) 1781.

[24] D.A. Bruce, A.P. Wilkinson, M.G. White, J.A. Bertrand, J. Solid State Chem. 125 (1996) 228.

[25] S. Oliver, A. Kuperman, A. Lough, G.A. Ozin, Inorg. Chem. 35 (1996) 6373.

[26] Q. Gao, B. Li, J. Chen, S. Li, R. Xu, J. Solid State Chem. 37 (1997) 129.

[27] A.M. Chippindale, A.R. Cowley, Q. Huo, R.H. Jones, A.D. Law, J. Chem. Soc. Dalton Trans. (1997) 2639.

[28] N. Togashi, J. Yu, S. Zheng, K. Sugiyama, K. Hiraga, O. Terasaki, W. Yan, S. Qiu, R. Xu, J. Mater. Chem. 8 (1998) 2827.

[29] L. Vidal, C. Marichal, V. Gramlich, J. Patarin, Z. Gabelica, Chem. Mater. 11 (1999) 2728.

[30] J. Yu, J. Li, K. Sugiyama, N. Togashi, O. Terasaki, K. Hiraga, B. Zhou, S. Qiu, R. Xu, Chem. Mater. 11 (1999) 1727.

[31] H. Yuan, G. Zhu, J. Chen, W. Chen, G. Yang, R. Xu, J. Solid State Chem. 151 (2000) 145.

[32] A. Tuel, V. Gramlich, Ch. Baerlocher, Microporous Mesoporous Mater. 41 (2000) 217.

[33] W. Yan, J. Yu, Z. Shi, R. Xu, Chem. Commun. (2000) 1431.

[34] A. Tuel, V. Gramlich, Ch. Baerlocher, Microporous Mesoporous Mater. 46 (2001) 57.

[35] A. Tuel, V. Gramlich, Ch. Baerlocher, Microporous Mesoporous Mater. 47 (2001) 217.

[36] W. Yan, J. Yu, Z. Shi, R. Xu, Stud. Surf. Sci. Catal. 35 (2001) 05-P-10.

[37] A. Tuel, V. Gramlich, Ch. Baerlocher, Microporous Mesoporous Mater. 56 (2002) 119.

[38] W. Yan, J. Yu, Y. Li, Z. Shi, R. Xu, J. Solid State Chem. 167 (2002) 282.

[39] L. Vidal, V. Gramlich, J. Patarin, Z. Gabelica, Eur. J. Solid State Chem. 35 (1998) 345.

[40] P. Feng, X. Bu, G.D. Stucky, Inorg. Chem. 39 (2000) 2.

[41] A. Tuel, V. Gramlich, Ch. Baerlocher, Microporous Mesoporous Mater. 47 (2001) 217.

[42] A. Tuel, J.L. Jorda, V. Gramlich, Ch. Baerlocher, J. Solid State Chem. 178 (3) (2005) 782.

[43] G.M. Sheldrick, SHELXTL PLUS, program for the solution of crystal structures, University of Göttingen, Germany, 1986.

[44] G.M. Sheldrick, SHELX 93, program for the refinement of crystal structures, University of Göttingen, Germany, 1993.

[45] A. Medek, J.S. Harwood, L. Frydman, J. Am. Chem. Soc. 117 (1995) 12779.

[46] C. Fernandez, J.P. Amoureux, J. Phys. Lett. 242 (1995) 449.

[47] D. Marion, K. Würthrich, Biochem. Biophys. Res. Commun. 113 (1983) 967.

[48] G. Drobny, A. Pines, S. Sinton, D. Weitekamp, D. Wemmer, Symp. Faraday Div. Chem. Soc. 13 (1979) 49.

[49] D. Müller, E. Jahn, G. Ladwig, U. Haubenreisser, Chem. Phys. Lett. 109 (1984) 332.